

# Friction Modifier Behaviour in Lubricated MEMS Devices

T. Reddyhoff · I. S. Y. Ku · A. S. Holmes ·  
H. A. Spikes

Received: 5 March 2010 / Accepted: 27 September 2010 / Published online: 13 October 2010  
© Springer Science+Business Media, LLC 2010

**Abstract** Low viscosity fluids could provide reliable lubrication for certain microelectromechanical system's (MEMS) applications where high-sliding speeds and/or high sliding distances occur. However, while the use of low viscosity fluids leads to reduced hydrodynamic friction, high boundary friction can be a significant issue at low entrainment speeds. This article describes a series of tests of low viscosity fluids, blended with a friction modifier additive so as to provide a combination of both low hydrodynamic and low boundary friction at MEMS scales. The low viscosity fluids tested were hexadecane, low viscosity silicone oil, toluene and water. With the exception of water, the addition of the organic friction modifier octadecylamine to all these lubricating fluids produced a significant reduction in boundary friction. For a MEMS contact lubricated with silicone oil for instance, boundary friction was reduced from 0.5 to close to 0.05. The presence of the amine dissolved in the toluene had the effect of reducing boundary friction from 0.75 to 0.55; this was further reduced to 0.25 after the specimens had been immersed in the toluene-additive blend for 48 h. A water-soluble additive, diethylamine, was added to de-ionized water, at 0.1% by weight concentration. Although an initial reduction in boundary friction was observed (0.45–0.25), under these conditions the rapid onset of severe wear negated these effects. It is suggested that corrosion of

silicon by water, followed by abrasion, is the cause of this accelerated wear.

**Keywords** Microelectromechanical systems · Boundary lubrication · Hydrodynamic lubrication · Additives · Friction modifiers

## 1 Introduction

Microelectromechanical systems (MEMS) have developed into a major technology, building on the success of the microelectronics industry over the past 50 years. MEMS technology is being incorporated into an increasing range of engineered products and its potential, both to enable new types of machines and instruments to be designed and to change the economics of existing ones, is likely to have a profound impact on our way of life over the next decades.

While many of the issues associated with engineering mm- and sub-mm-sized devices have been resolved, the lubrication of contacting and sliding parts at these scales remains a significant challenge [1]. This is because of the relatively large surface area to volume ratio, which results in surface forces outweighing the effects of inertia. In low sliding applications, such as micro-switches and positioners, this scaling effect leads to stiction, where the applied force is not sufficient to overcome surface adhesion and the capillary action of condensed water. This problem has been partly overcome through the application of surface coatings of inorganic and fluorinated organic compounds [2, 3].

The problem of dynamic friction and wear, present in high sliding MEMS, has proved much more difficult to solve. Despite the appeal of high functionality at low cost provided by miniature gears, linear racks, rotating platforms and pop-up mirrors, no MEMS devices incorporating sliding

---

T. Reddyhoff (✉) · I. S. Y. Ku  
Tribology Group, Department of Mechanical Engineering,  
Imperial College, London SW7 2AZ, United Kingdom  
e-mail: t.reddyhoff@imperial.ac.uk

A. S. Holmes · H. A. Spikes  
Optical and Semiconductor Devices Group, Department  
of Electrical and Electronic Engineering, Imperial College,  
London SW7 2AZ, United Kingdom

contacts have yet been commercialized [4]. The ‘dry’ methods mentioned above effectively provide more hydrophobic surfaces to reduce the effects of surface forces. However, they often become unstable or damaged during prolonged use. To operate for extended periods with high amounts of sliding, lubrication methods are required that replenish and thus repair the protective layers on the surfaces as these become damaged. This requirement for self-replenishment has been recognized in only a few studies at the MEMS scale. One recent example has been the replenishment from the vapour phase of the lubricant film in a MEMS device [5, 6]. Here a volatile alcohol is vaporized so as to condense on the rubbing surfaces during operation. The film thus formed is very thin and tribologically similar to that formed from liquid deposition [7]. Alcohol molecules that attach to the surface in this way have been shown to provide excellent wear resistance in MEMS contacts.

An alternative approach with the potential for self-replenishment is liquid lubrication. Liquids are often presumed to produce excessive drag and deemed unsuitable for lubricating MEMS. However, only a very limited amount of literature has been published on the subject. In a study using predominantly silicone oil it was found that the maximum operating speeds of electrostatic micromotors were restricted as a result of the drag from the liquid [8]. The effects of drag were also found to cause over-damping in salient-pole micromotors, when lubricated by a range of silicone oils with viscosities from 20 to 60 centistokes [9]. Unfortunately this latter study used quite high viscosity liquids and it is probable that the problems of excessive drag could have been alleviated simply through the use of lubricating fluids of lower viscosity.

Recently the authors have shown, using a custom-built tribometer [10], that acceptably low friction can be achieved in MEMS sliding contacts lubricated by liquids provided the lubricants are of sufficiently low viscosity. It has also been demonstrated that drag forces can be very low for sliding contacts submerged in low viscosity liquids. At low speeds, however, where hydrodynamic entrainment is insufficient to separate the sliding surfaces, unacceptably high boundary friction is observed. In this article it is demonstrated that, by blending such low viscosity fluids with appropriate boundary additives, it is possible to achieve low hydrodynamic friction without the penalty of high boundary friction. In this lubrication scheme, part of the boundary film may be removed during sliding, but when this happens the film is replenished by the free surfactant in the lubricant [11]. For the effective boundary lubrication of silicon-based MEMS, additives able to adsorb or react to form protective films on silicon or silicon oxide are required. To date, self-replenishing boundary films in MEMS have been achieved only through delivery from the vapour phase, as described above.

The possibility of using liquids to act as carriers for boundary lubricant additives appears to have been wholly ignored in MEMS research to date, and the few previously published studies of liquid-lubricated MEMS have used additive-free fluids. However, it is well known in macro-scale tribology that the role of liquids as suppliers of boundary lubrication is at least as important as their hydrodynamic role. This implies that there may be a valuable role for liquid lubrication even in low-speed MEMS, particularly in devices where maintenance of a low friction sliding contact over very long periods is important.

## 2 Experimental Details

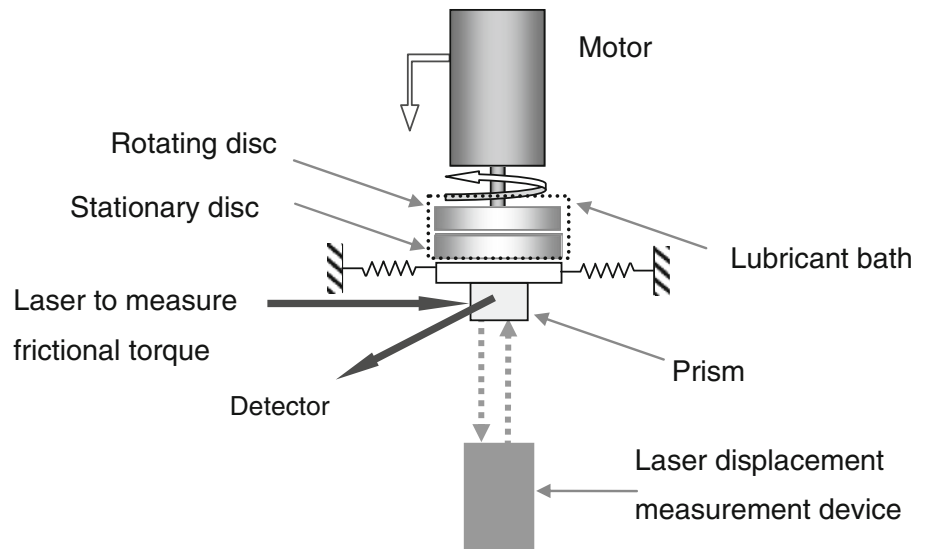
### 2.1 Test Rig

The microtribometer used in this work to test high-sliding contacts under real MEMS conditions is similar to that described by Ku et al. [10]. A schematic of the apparatus is shown in Fig. 1. Frictional torque is measured between the surfaces of two silicon disc specimens. The lower specimen is stationary and mounted on a platform supported by an elastic suspension of known torsional and normal stiffness. The upper specimen is attached to the shaft of a high-speed DC motor, the height of which may be adjusted via a computer-controlled vertical stage.

At the start of each test, the motor is lowered until the specimens are in contact and under the required normal load. The normal load is determined from the vertical position of the platform. A laser displacement measurement device located beneath the platform is used to measure its vertical position, from which the normal force is calculated using the known vertical stiffness of the suspension. The suspension stiffness is determined beforehand by placing small known weights on the platform and measuring the resulting displacements.

The frictional torque is determined by measuring the rotation of the platform. Since forces and therefore displacements are small, an optical lever technique is used. Here, a laser beam is incident on a small prism bonded to the underside of the platform. The laser beam subsequently reflects off a piezoelectric actuator, followed by four mirrors, before being incident on a light-sensitive detector. A feedback loop is implemented such that the actuator rotates to ensure that the laser beam is always incident on the centre portion of the detector. Then, as the frictional torque from the contact causes the platform to rotate, the voltage signal to the actuator is proportional to the angle of rotation. The four mirrors are used to maximize the length of the light path and thus increase sensitivity. The voltage signal to the actuator is calibrated to the rotation of the platform by varying the position of the detector. The

**Fig. 1** Schematic of the microtribometer



frictional torque is then found from the platform rotation and its angular stiffness. The platform stiffness is found by applying a known torque using a custom-built device consisting of two small beams with strain gauges attached. The measured stiffness from the torque device is confirmed by simple beam theory calculations.

The upper and lower specimens are submerged in a small, glass lubricant bath. Both the motor stage and the platform are positioned using two-axis horizontal stages. Alignment of the specimens is enabled by two video camera microscopes that view the contact from different directions. Figure 2 shows a still image from one of the cameras once the contact is submerged in lubricant.

For all the tests in this study, the motor was lowered until the platform was displaced vertically by  $2.2\ \mu\text{m}$ , corresponding to a load of  $0.05\ \text{N}$ . The motor was then spun up to a known speed and the angular displacement of the platform was measured to determine the frictional

torque. The acquisition of data and control of the motor were automated to allow the curves of friction coefficient versus rotational speed to be obtained.

## 2.2 Test Platforms and Specimens

As shown in Fig. 3, the test platform consists: (1) an inner platform supported by several thin radial beams (torsional springs) which provide the torsional flexibility, and (2) an outer platform supported by four folded flexure beams (normal load springs) with low out-of-plane stiffness. The inner platform has features for locating the lower disc specimen; it also carries the lubricant bath on its top surface and the prism on its underside, and has additional silicon features that act as mechanical stops to prevent over-rotation. The flexures on the outer platform link to an overall supporting frame. The platforms were fabricated on 100-mm diameter, 525- $\mu\text{m}$  thick silicon wafers by a combination of photolithography and through-wafer deep reactive ion etching (DRIE). This fabrication approach allows several test platforms with varying geometries to be fabricated at one time. All designs had an overall footprint of  $25 \times 25\ \text{mm}$ .

The silicon disc specimens were also fabricated by photolithography and DRIE. For all tests the upper, rotating specimen was flat, while the lower, stationary specimen was textured with a pattern similar to that of a stepped pad bearing. The pattern was etched to a depth of  $50\ \mu\text{m}$  and had dimensions as shown in Fig. 4. Additional features were etched in the specimens to allow them to be located on the test platform or motor shaft.

## 2.3 Test Lubricants

The following low viscosity liquids were tested: low viscosity silicone oil (polydimethylsiloxane), hexadecane,

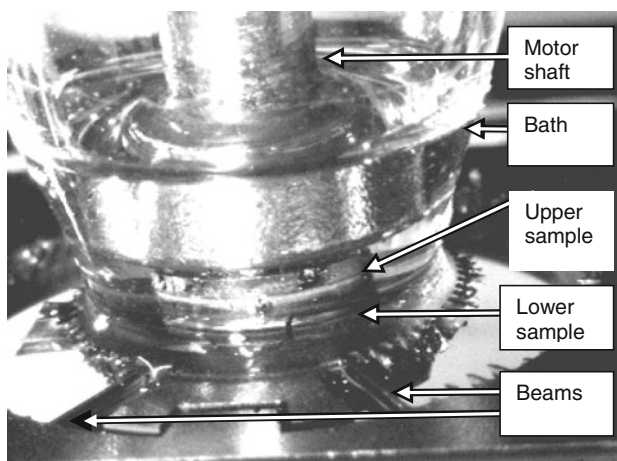


**Fig. 2** Still image from one of the video cameras showing a close-up of the two specimens in contact

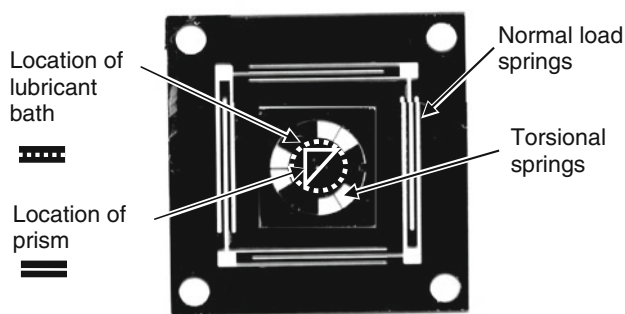


**Fig. 3** Photograph of a silicon test platform

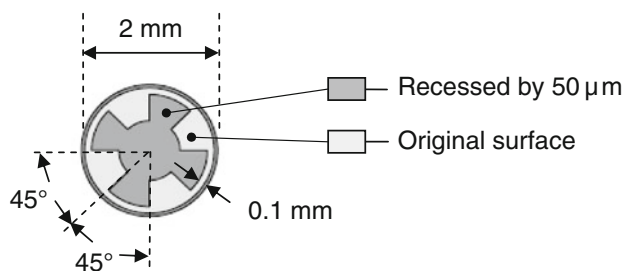


**Fig. 4** Schematic showing design and dimensions of lower disc specimen

toluene and deionised (DI) water. The dynamic viscosities and densities of these liquids at 25 °C are listed in Table 1.

#### 2.4 Friction Modifier Additives

Organic friction modifier (FM) additives conventionally consist of a molecule with a polar head group which is attracted to a polar surface and a hydrocarbon tail which is soluble in the oil [12]. The rapid formation of a FM film on a steel surface occurs due to a combination of cohesion between the surface active head group and the surface and intermolecular forces present between the alkyl chains in the film.

Additives with amine head groups have been shown to be attracted to mica surfaces in a surface force apparatus [13]. Here it is suggested that the amine head group is adsorbed on the sliding surfaces and forms a disordered single layer, reducing static friction and limiting the shear

**Table 1** Properties of lubricants at 25 °C

Lubricants	Dynamic viscosity $\eta$ (cP)	Density $\rho$ (g/cm <sup>3</sup> )
Silicone oil	0.880	0.8147
Hexadecane	3.032	0.7733
Toluene	0.605	0.8625
Water	0.890	0.997

Values were measured using a Stabinger Viscometer (modal SVM 3000, Anton Paar, Graz, Austria)

stress. The similarity between mica and silica suggested that an amine additive should function as an effective FM in the current work.

For the two lubricants silicone oil and toluene, the additive octadecylamine,  $\text{CH}_3(\text{CH}_2)_{17}\text{NH}_2$ , was used at a concentration of 0.1 wt%. The amine dissolved easily in toluene at room temperature, but to dissolve the additive in silicone oil, the base fluid was heated to 60 °C before addition of the amine. The blend was then allowed to cool before tests were carried out. Octadecylamine was poorly soluble in water due to its long chain length, therefore the shorter dodecylamine,  $\text{CH}_3(\text{CH}_2)_{11}\text{NH}_2$ , was used. This reduction in FM chain length from eighteen to twelve is likely to reduce the friction modifier's effectiveness, since fewer interactions will occur between shorter adsorbed molecules, which inhibit surface contact (see for example [14]).

Common friction modifiers used with metal surfaces, for instance fatty acids such as palmitic and stearic acid, are generally soluble in the low viscosity fluids studied, but are weakly attracted to silica surfaces.

### 3 Results and Discussion

Testing was carried out using the miniature step bearing geometry. All tests were carried out at room temperature ( $24 \pm 1.5$  °C). The following results are displayed as Stribeck curves of friction measurements from the contact between a flat upper specimen and the stepped pad shown in Fig. 4.

#### 3.1 Silicone Oil

Figure 5 shows how friction varies with speed for the contact lubricated with silicone oil. The log scale plot, shown in part b of the figure, highlights low speed behaviour. For neat silicone oil, boundary friction of  $\sim 0.5$  occurs, which then falls with increasing speed as a hydrodynamic film forms to separate the surfaces. The addition of 0.1% octadecylamine blended with the silicone oil reduces boundary friction to  $\sim 0.05$  at low speeds. This friction increases with speed. It is well known that boundary friction of organic friction modifiers can increase with sliding speed and this has been explained in terms of an activated shear model [15]. The lower friction at very low speed with silicone oil is possibly due to the presence of a hydrated or otherwise contaminated silica film that is rapidly removed. At speeds of ca 3000 rpm the friction of the additive solution approaches that of the neat silicone oil. This suggests that, once surfaces are fully separated, the adsorbed amine does not significantly affect the lubrication mechanism. Thus no slip at the wall occurs as a

result of the adsorbed layer, as has been shown previously [16, 17]. To indicate repeatability, results from two separate tests are shown in Fig. 5a.

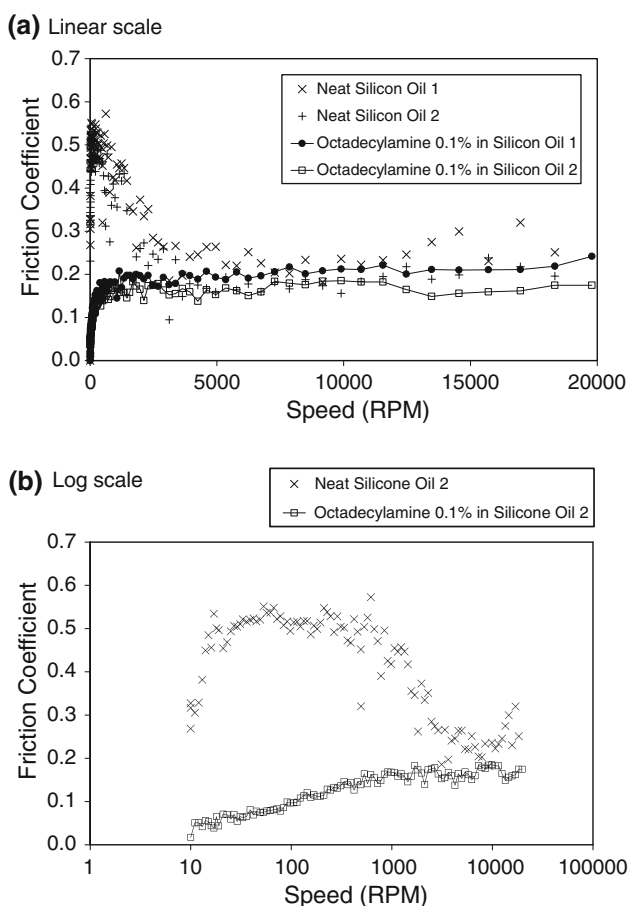
### 3.2 Hexadecane

Figure 6 shows friction/speed curves when the contact is lubricated with hexadecane and with a solution of the long chain amine in hexadecane. The log plot for neat hexadecane (Fig. 6b) clearly shows a minimum occurring around 3000 rpm; at this speed film thickness is sufficient to separate the surfaces, but low enough to minimize viscous shear. The presence of the dissolved octadecylamine dramatically reduces the boundary friction from ~0.25 down to a value close to zero. At the speed where the neat hexadecane friction is a minimum, the amine blend shows a change in gradient. This change in gradient is due to the change in lubrication regime from boundary (albeit with modified friction) to hydrodynamic. As the speed increases beyond this point, both the blend and the neat hexadecane give the same friction. The friction curves obtained from hexadecane show less noise than

those obtained for other lubricants. The reason for this is possibly that the higher viscosity of hexadecane produces a damping effect.

### 3.3 Toluene

Figure 7 shows how friction coefficient varies with speed for a contact lubricated with pure toluene. Part (a) of the figure shows the two sets of data for each test condition (again showing repeatability). Part (b) shows one set of data for each condition plotted on log scale to show more clearly the friction behaviour at low speeds. When lubricated with neat toluene, friction begins at ~0.75 at very low speed and reduces with increasing speed as a fluid film is built up. Addition of 0.1% octadecylamine to the lubricant initially reduces the boundary friction to 0.55. However, if the contact is left submerged in the toluene–amine blend for 48 h and the test repeated, boundary friction is reduced still further to a value close to 0.25. This reduction in friction when the silicon surfaces are left exposed to the amine, suggests that an ordered surface film is gradually being formed on the surface. This reduction in friction due to extended submersion was observed only when toluene



**Fig. 5** Friction coefficient versus speed for contact lubricated with silicone oil, showing the effect of octadecylamine

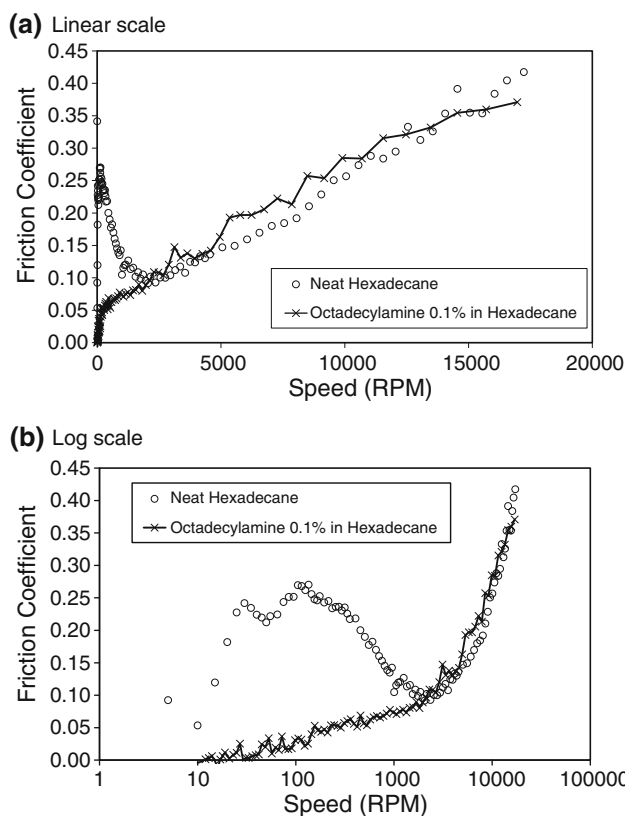


**Fig. 6** Friction coefficient versus speed for contact lubricated with hexadecane, showing the effect of octadecylamine

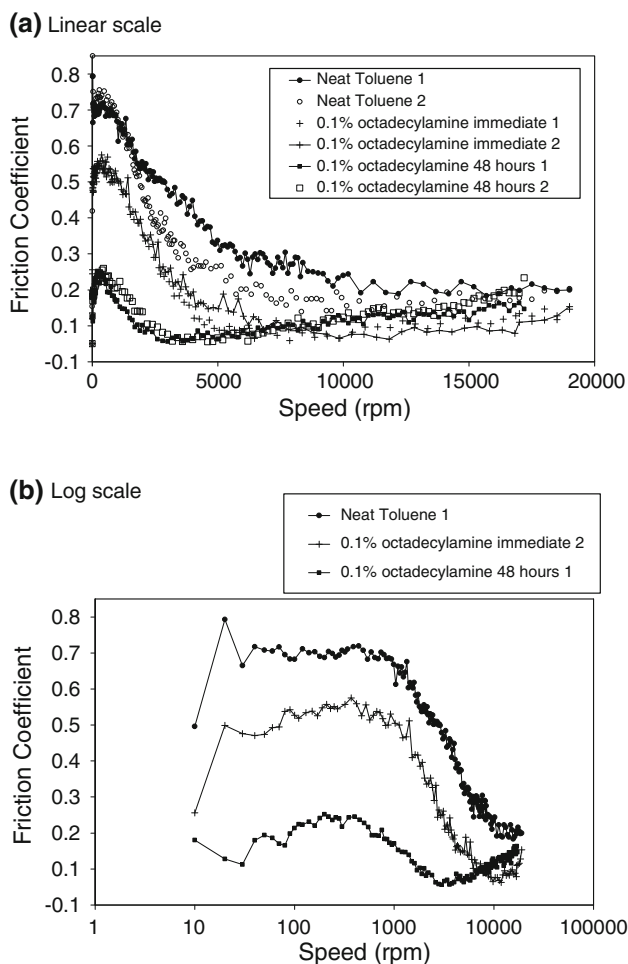


**Fig. 7** Friction coefficient versus speed for contact lubricated with toluene, showing the effect of octadecylamine

was used as the base fluid, perhaps because toluene competed with the amine for the silicon/silica surface so that an amine film took longer to self-assemble.

### 3.4 Water

The possibility of using water with a boundary lubricating additive was also explored. A water-soluble additive, dimethylamine was added to DI water at 0.1% by weight concentration. Figure 8 shows how the coefficient of friction varied with speed for the cases of pure DI water and additive dissolved in pure DI water.

With pure DI water, the friction coefficient is initially about 0.1 at very low speed but then increases rapidly to peak at 0.5 before reducing drastically at high speed. It is believed that a low friction film, possibly of hydrated silica, is present initially which is rapidly removed so that the value of 0.5 represents the steady state boundary friction coefficient value of silicon/silicon in a water/air environment. Friction then decreases at high speeds as a hydrodynamic

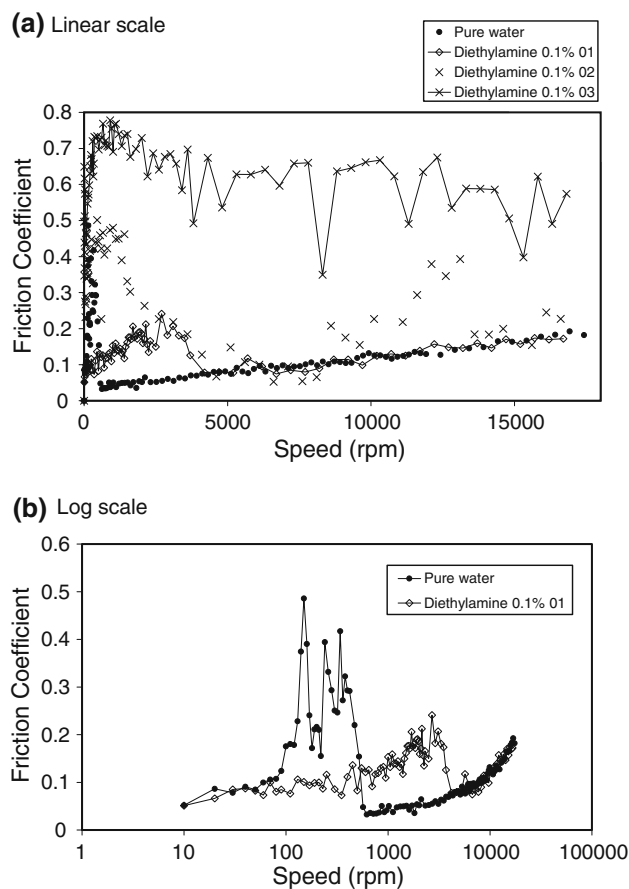


**Fig. 8** Friction coefficient versus speed for contact lubricated with water, showing the effect of diethylamine

water film in generated to separate the surfaces. Three successive tests with the solution of dimethylamine dissolved in pure DI water were run. In the first test run, the maximum friction was reduced to 0.25; however, the boundary friction appeared to persist up to a speed of around 4000 rpm. Then, as speed increased further friction decreased to follow the same trend in the hydrodynamic region as that for water. The next two runs, however, both showed friction coefficients that increased greatly in the low speed region. This behaviour is believed to originate from the accumulation wear debris from the silicon surfaces that occurs in the presence of water. As the surfaces wear, roughness increases and boundary friction is prevalent. Wear is accelerated by the presence of water, which acts to corrode the silicon surfaces to form an easily abraded hydrated silica film.

The corrosion of silicon surfaces due to the presence of liquid water has been observed and explained in work carried out by Graf et al. [18]. The corrosion process occurs as water acts to breaks the Si–Si bonds after first being dissociatively chemisorbed on its surface. The reaction produces  $\text{SiO}_2$ , which due to altered surface topography

and strain within the silicon, grows at a non-uniform rate. The oxide formation is accompanied by a slight corrosive attack of H<sub>2</sub>O leading to a roughening of the surface. A detailed outline of the steps involved in this reaction is given in [18].

### 3.5 The Silicon Surface

Within the boundary lubrication regime, load is supported by asperity–asperity contact, and friction arises from the shearing of these conjunctions. Boundary additives can then adsorb onto the asperity surfaces to form thin layers to reduce asperity contact and therefore shear stress. The composition of the silicon surfaces before sliding therefore plays a role in determining the boundary lubrication behaviour. The final stage of fabrication of the silicon specimen involves a chemical etch, which removes all silicon dioxide (silica) from the surface to leave only silicon exposed. However, this condition does not last for long since only a silicon crystal that is cleaved in ultrahigh vacuum exhibits a surface free of other elements [19]. Even at room temperature, once exposed to air a ‘native oxide film’ grows rapidly [20]. Silicon dioxide films formed in this way have been measured using SEM and shown to be of the order of 2–3 nm thick [21]. Without elevated temperatures, subsequent growth of the oxide film is hindered since molecules of oxygen required to form the film must penetrate the existing oxide to reach the underlying silicon.

Silica is an acidic oxide, which may explain why fatty acids such as stearic acid are not very effective as FMs for silicon components, since limited attraction occurs between the oxide surface and the carboxylic acid molecules (This is not necessarily the case for fatty acid salts). However, amines with their weakly alkaline head group can bind well with silica surfaces, and therefore act as friction modifiers.

## 4 Conclusions

In this work friction was measured for a range of low viscosity lubricants in order to demonstrate the ability of an amine additive to reduce friction in MEMS contacts at low speed. The results of these experiments are summarized as follows:

- For the low viscosity lubricants silicone oil, toluene, hexadecane, the addition of 0.1 wt% octadecylamine, resulted in an immediate and significant reduction in boundary friction.
- The toluene–octadecylamine blend showed a further reduction in friction after samples were left submerged for a period of 48 h. This may be due to competition from the toluene molecules for the silicon/silica surface impeding the self-assembly of the amine monolayer.

- The addition of diethylamine to de-ionized water resulted in an initial reduction in boundary friction from 0.45 to 0.25. However, this effect was curtailed by the rapid onset of severe wear of the silicon surfaces.
- Stearic acid was blended with the lubricants tested and, although soluble, showed no reduction in friction. This may be because of lack of strong adsorption of carboxylic acid groups on silicon dioxide surfaces.

In light of the findings presented, it is believed that lubrication by boundary additives in low viscosity liquids may provide a very robust and versatile method for lubricating MEMS.

**Acknowledgments** The financial support of the UK Engineering and Physical Sciences Research Council (EPSRC) under Grant No. EP/D04099X is gratefully acknowledged. The authors also wish to thank Mr. Robert J. Hergert of the Optical and Semiconductor Devices Group at Imperial College for his help with the design and fabrication of the test devices used in this work, and other members of the Optical and Semiconductor Devices and Tribology Groups at Imperial College for their assistance.

## References

1. Spearing, S.M.: Materials issues in microelectromechanical systems (MEMS). *Acta Mater.* **48**, 179–196 (2000)
2. de Boer, M.P., Mayer, T.M.: *Tribol. MEMS. MRS Bull.* **26**(4), 302–304 (2001)
3. Maboudian, R., Ashurst, W.R., Carraro, C.: Self-assembled monolayers as anti-stiction coatings for MEMS: characteristics and recent developments. *Sens. Actuators* **82**, 219–223 (2000)
4. Sniegowski, J.J., de Boer, M.P.: IC-compatible polysilicon surface micromachining. *Ann. Rev. Mater. Sci.* **30**, 299–333 (2000)
5. Asay, D.B., Dugger, M.T., Kim, S.H.: In situ vapor-phase lubrication of MEMS. *Tribol. Lett.* **29**(1), 67–74 (2008)
6. Asay, D.B., Dugger, M.T., Ohlhausen, J.A., Kim, S.H.: Macro- to nanoscale wear prevention via molecular adsorption. *Langmuir* **24**, 155–159 (2008)
7. Ashurst, W.R., Carraro, C., Maboudian, R.: Vapor phase anti-stiction coatings for MEMS. *IEEE Trans. Device Mater. Reliab.* **3**(4), 173–178 (2003)
8. Mehregany, M., Dhuler, V.R.: Operation of electrostatic micromotors in liquid environments. *J. Micromech. Microeng.* **2**, 1–3 (1992)
9. Deng, K., Ramanathan, G.P., Mehregany, M.: Micromotor dynamics in lubricating fluids. *J. Micromech. Microeng.* **4**, 266–269 (1994)
10. Ku, I.S.Y., Reddyhoff, T., Choo, J.H., Holmes, A.S., Spikes, H.A.: A novel tribometer for the measurement of friction in MEMS. *Trib. Int.* **5–6**, 1087–1090 (2010)
11. Stackowiak, G.W., Batchelor, A.W.: *Engineering tribology*, Second edn. Butterworth Heinemann, Need City (1993)
12. Mortier, R.M., Orszulik, S.T.: *Chemistry and technology of lubricants*, Second edn. Blackie Academic and Professional, London (1997)
13. Zhu, X., Ohtanib, H., Greenfield, M.L., Ruths, M., Granicka, S.: Modification of boundary lubrication by oil-soluble friction modifier additives. *Tribol. Lett.* **15**(2), 127–134 (2003)
14. Jahanmir, S.: Chain length effects in boundary lubrication. *Wear* **102**, 331–349 (1985)

15. Briscoe, B.J., Evans, D.C.B.: The shear properties of Langmuir-Blodgett layers. *Proc. Roy. Soc. Lond. A* **380**, 389–407 (1982)
16. Choo, J.H., Spikes, H.A., Ratoi, M., Glovnea, R., Forrest, A.K.: Friction reduction in low-load hydrodynamic lubrication with a hydrophobic surface. *Trib. Int.* **40**, 154–159 (2007)
17. Choo, J.H., Glovnea, R.P., Forrest, A.K., Spikes, H.A.: A low friction bearing based on liquid slip at the wall. *Tribol. Trans. ASME J* **129**, 611–620 (2007)
18. Graf, D., Grundner, M., Schulz, R.: Reaction of water with hydrofluoric acid treated silicon (111) and (100) surfaces. *J. Vac. Sci. Technol. A* **7**(3), 808–813 (1988)
19. Lehmann, V.: *Electrochemistry of silicon: instrumentation, science, materials and applications*, First edn. Wiley-VCH, Weinheim (2002)
20. Law, T.J.: Interaction of oxygen with clean silicon surfaces. *J. Phys. Chem. Solids* **4**, 91–100 (1958)
21. Gavrilenko, V.P., Novikov, Yu.A., Rakov, A.V., Todua, P.A.: Measurement of thickness of native silicon dioxide with a scanning electron microscope. *Proc. SPIE* **7405**, 7–8 (2009)